ACS APPLIED ENERGY MATERIALS

www.acsaem.org Article

Silicon Layer on Polymer Electrolyte as a Dendrite Stopper for Stable Lithium Metal Batteries

Li Zhao, Lulu Du, Hantao Xu, Jiahui Deng, and Lin Xu*

Cite This: ACS Appl. Energy Mater. 2023, 6, 9523−9531 Read Online

ACCESS | Metrics & More | Article Recommendations | Supporting Information

ABSTRACT: Silicon (Si) is a promising candidate for next-generation anode materials because of its high specific capacity of 3579 mAh g^{-1} and low potential of 0.4 V (vs Li^+/Li). However, the development of Si anode has been limited by the huge volume expansion during the lithiation process. Here, a layer of core−shell Si@SiO_x nanoparticles is coated on one surface of the polymer electrolyte as a dendrite stopper by taking advantage of the high specific capacity of Si, and the negative effects of Si volume expansion can be offset by the flexibility of the polymer electrolyte. The Si@SiO_x layer is employed to match the lithium metal anode for suppressing the growth of lithium dendrites. When lithium dendrites are in contact with the Si@SiO_x layer, the Si@SiO_x nanoparticles can react with lithium ions deposited on the contact interface to form a Li−Si alloy (Li_ySi), which can reduce the concentration of lithium ions at the sharp ends of lithium dendrites, thus inhibiting the further growth of lithium dendrites. As a result, symmetric Li//Li cells can maintain stability without lithium dendrites for more than 2600 h. This study presents a promising approach to address the dendrite issue in solid-state lithium metal batteries.

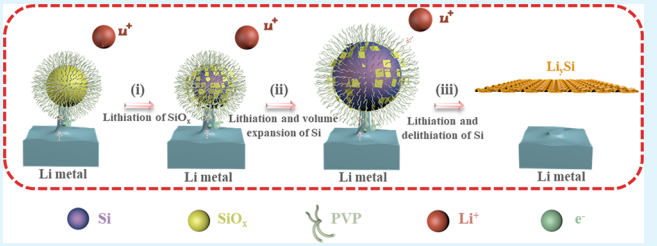

KEYWORDS: *polymer electrolytes, Si@SiO_x layer, alloying reaction, lithium dendrites, lithium metal batteries*

1. INTRODUCTION

Lithium-ion batteries are widely utilized in digital devices, electric vehicles, and energy storage systems due to their high energy density, extended life span, and low self-discharge rate.[1−3] However, safety hazards derived from electrolyte leakage and dendrite growth remain significant concerns.[4,5] Compared with liquid lithium-ion batteries, quasi-solid lithium metal batteries with a lower content of liquid electrolytes can effectively avoid electrolyte leakage.[6,7] However, the formation of lithium dendrites caused by nonuniform lithium-ion deposition still remains a challenge for quasi-solid lithium metal batteries.[8−10] To address the dendrite issue, artificial coatings are designed at the interface between polymer electrolytes and lithium metal anodes to promote uniform lithium-ion deposition.[11,12]

Commonly, artificial coatings are applied to the surface of lithium metal to form alloys for the uniform deposition of lithium ions.[13,14] One such artificial coating is tin fluoride (SnF_2) on the surface of lithium metal, which reacts with lithium metal to form a tin−lithium alloy (Li_5Sn_2) for the uniform deposition of lithium ions.[15] Additionally, a thin metal-tungsten interlayer on the surface of lithium metal has been demonstrated to facilitate the uniform deposition of lithium ions through a lithium−tungsten alloying reaction.[16−18] However, the softness of the lithium metal surface, the complex fabrication process, and strict environmental requirements severely hinder the development of artificial coatings on the surface of the lithium metal. Therefore, the construction of artificial coatings on polymer electrolytes has been a better choice.[19−21] In general, polymer electrolytes display insufficient mechanical strength to resist the growth of lithium dendrites.[22] An effective approach to resist dendrite growth is to construct artificial coatings on the surface of polymer electrolytes for uniform lithium-ion deposition.

Si or SiO_x has been reported to enable stable interfaces on the surface of lithium metals through alloying reactions. In previous reports, Si or SiO_x has mainly been used as an anode material.[22,23] For example, Li_ySi particles were evenly distributed to form a porous 3D Li−Si alloy-type interfacial framework, which was utilized by in situ spontaneous prelithiation of Si. This framework provides balanced ionic and electronic conductivity, acting as a stable Li host and preventing dendrite growth and volume expansion during cycling.[22,24,25] Moreover, the alloying reaction between SiO_x and the lithium metal produces Li_ySi, which forms a stable interface.[26] Si is oxidized to form SiO_x, which can subsequently serve as a core−shell structure with Si@SiO_x. The surface of

Received: June 15, 2023
Accepted: August 24, 2023
Published: September 1, 2023

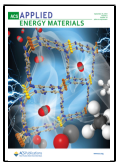

https://doi.org/10.1021/acsaem.3c01498
ACS Appl. Energy Mater. 2023, 6, 9523−9531

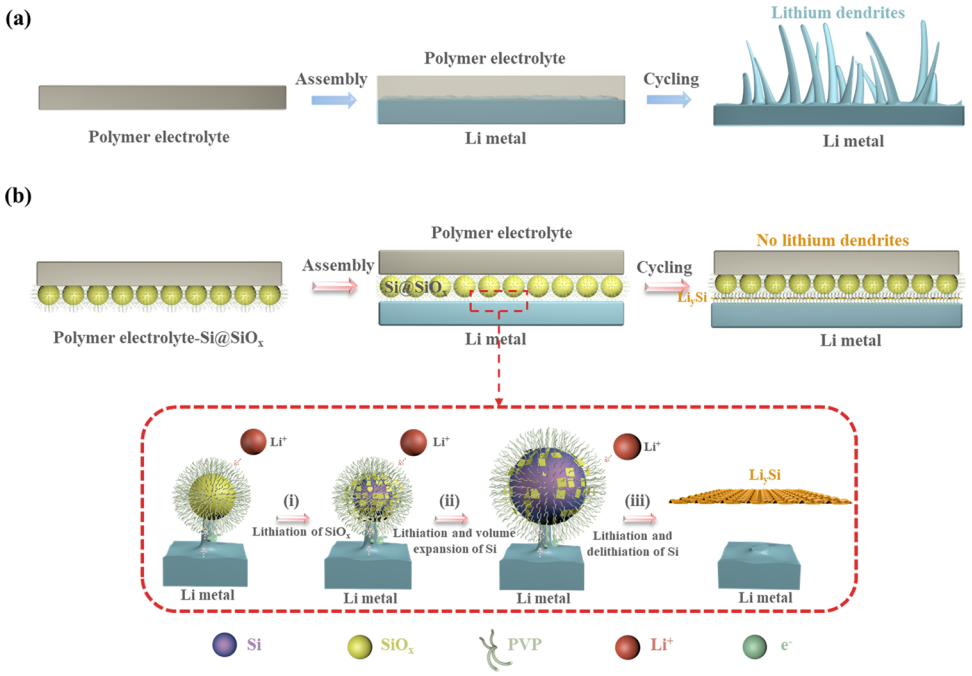

Figure 1. Schematic illustration of Si@SiO_x as a lithium dendrite stopper. (a) Polymer electrolyte. (b) Polymer electrolyte-Si@SiO_x. (i) Deposited lithium ions react with SiO_x to form Li_ySi and Li_ySiO_x. (ii) Si reacts with the lithium ions deposited at the contact interface to form Li_ySi, which causes volume expansion. (iii) Further alloying reactions occur to form a layer of Li−Si alloy.

the structure is primarily composed of SiO_x and remains a stable interface. However, Si@SiO_x has never been employed as a functional coating for polymer electrolytes.[27,28] Using Si@SiO_x as a polymer electrolyte coating will produce unexpected results. The Si@SiO_x nanoparticles with high specific capacity accommodate a large number of lithium ions, balancing the lithium-ion concentration for a stable interface to inhibit the growth of lithium dendrites.

Here, we design a layer of Si@SiO_x nanoparticles with a core−shell structure on one surface of the polymer electrolyte (polymer electrolyte-Si@SiO_x) to inhibit the growth of lithium dendrites. The Si@SiO_x nanoparticles are created by oxidizing Si nanoparticles with a layer of SiO_x to prevent the reaction with liquid electrolytes. To avoid the reaction between the Si@SiO_x nanoparticles and the lithium metal, a layer of polyvinyl pyrrolidone (PVP) is coated on the surface of Si@SiO_x nanoparticles. Then, the layer of Si@SiO_x is employed to match the lithium metal anode which reacts with lithium ions to form Li_ySi through an alloying reaction for dendrite suppression. Furthermore, the symmetric Li//Li cells can maintain stability for more than 2600 h at 0.1 mA cm^{-2}, and there are no lithium dendrites formed on the surface of the lithium metal after cycling.

2. EXPERIMENTAL SECTION

2.1. Synthesis of Polymer Electrolyte-Si@SiO_x. The preparation of polymer electrolyte-Si@SiO_x was done by adding PVDF-HFP and PEO in a 10:1 mass ratio to a sample bottle. Next, ethanol (1 mL) and DMF (8 mL) solution were added, and the resulting solution was magnetically stirred at 60 °C for 24 h. Subsequently, the solution was dissolved, and half of it was poured into a dish on a glass surface to form a film. The film was then transferred to an 80 °C drying oven. Meanwhile, Si and PVP were added in a mass ratio of 7:1 to a sample tube, followed by the addition of ethanol (2 mL). The solution was sonicated for 24 h until it was uniformly dispersed. Once the solvents of PVDF-HFP and PEO had volatilized, the dispersive solution was added to the surface and spread evenly before being put into an 80 °C air-drying oven. Once all the solvents had volatilized, the resulting material was transferred to a 60 °C vacuum-drying oven for 24 h. It was then removed, cut to a specified size, and placed in the air by a 60 °C drying oven for another 24 h. The liquid electrolyte is added to the specified size polymer electrolyte when it is placed on the surface of the lithium metal. The polymer electrolyte can quickly absorb the liquid electrolyte to form a quasi-solid polymer electrolyte containing $LiPF_6$. The final product obtained from this process is polymer electrolyte-Si@SiO_x.

2.2. Characterization of the Physicochemical Properties of Polymer Electrolyte-Si@SiO_x. X-ray diffraction (XRD) patterns were obtained using a D8 Discover X-ray diffractometer equipped with Cu Kα radiation. The morphology of polymer electrolyte-Si@SiO_x was characterized using a field-emission scanning electron microscope (JEOL-7100F) after gold coating. Energy-dispersive X-ray spectroscopy (EDS) was performed using an Oxford IE250 system. Transmission electron microscopy (TEM) images were captured with a JEM-1400plus instrument, while TEM and high-resolution TEM (HRTEM) images were acquired with a JEM-2100F microscope. Polymer electrolyte-Si@SiO_x was identified by X-ray photoelectron spectroscopy (XPS) using an ESCALAB 250Xi instrument.

2.3. Cell Assembly. Symmetric Li//Li cell: A polymer electrolyte with a diameter of 17 mm is interposed between two lithium metals with a diameter of 14 mm, followed by the addition of 30 μL commercial electrolyte to form a symmetric Li//Li cell.

Full battery: The cathode slurry was prepared using NMP solvent, with $LiFePO_4$, acetylene black, and PVDF mixed uniformly in a mass ratio of 7:2:1. A positive electrode sheet with an area density of approximately 1.3 mg cm^{-2} was obtained after coating. The 17 mm polymer electrolyte-Si@SiO_x was then placed on top of the 14 mm lithium sheet, and 30 μL of commercial electrolyte was added dropwise. Next, a 10 mm single-sided $LiFePO_4$ positive sheet was layered on top of the polymer electrolyte-Si@SiO_x surface, and a 15.8 mm steel sheet was pressed on top to encapsulate the structure.

3. RESULTS AND DISCUSSION

A layer of Si@SiO_x is employed to match the lithium metal anode for suppressing the growth of lithium dendrites (Figure 1). Lithium dendrites are formed due to the nonuniform

https://doi.org/10.1021/acsaem.3c01498
ACS Appl. Energy Mater. 2023, 6, 9523−9531

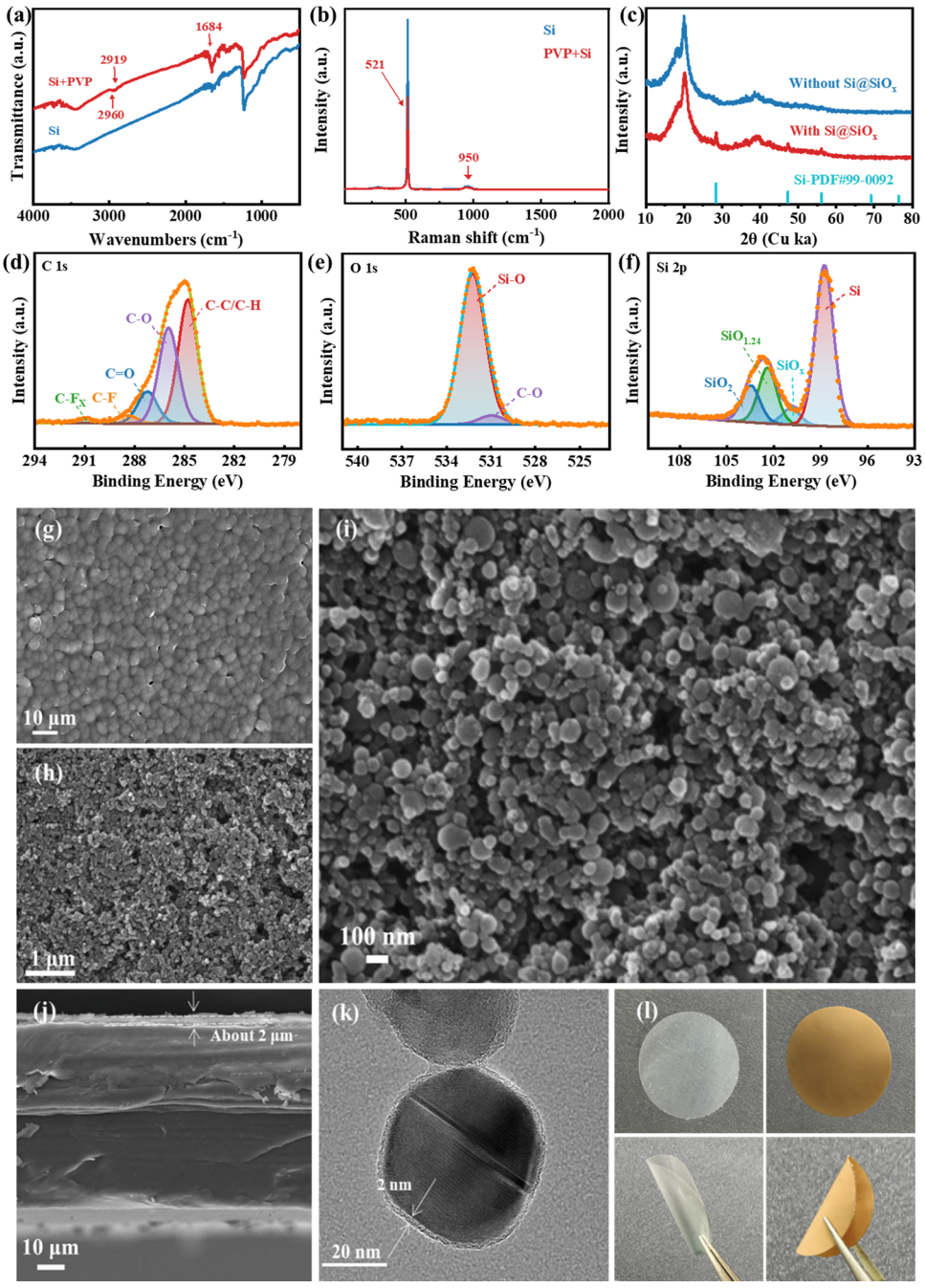

Figure 2. Characterizations of Si@SiO_x layers. (a) Infrared spectra of Si coated with PVP. (b) Raman spectra of Si coated with PVP. (c) XRD patterns of polymer electrolyte-Si@SiO_x. (d–f) XPS spectra of the (d) C 1s, (e) O 1s, and (f) Si 2p core regions of polymer electrolyte-Si@SiO_x. (g) SEM image of the polymer electrolyte. (h), (i) SEM images of polymer electrolyte-Si@SiO_x. (j) Cross-sectional SEM image of polymer electrolyte-Si@SiO_x. (k) TEM image of Si coated with PVP. (l) Photos of polymer electrolyte-Si@SiO_x being flat, bent, and after cycling.

deposition of lithium ions. When these lithium dendrites puncture the PVP layer and come into contact with the Si@SiO_x layer, the deposited lithium ions first react with the exterior SiO_x shell to form Li_ySi and Li_ySiO_x. However, the SiO_x shell is insufficient to control the rate of lithium deposition, especially at high current densities. Afterward, the interior Si core reacts with lithium ions deposited at the contact interface to form Li_ySi, which helps to control the rate of lithium-ion deposition. Because of the high theoretical specific capacity, the interior Si core can combine with more lithium ions during alloying reactions. Therefore, the Si@SiO_x layer can effectively inhibit the growth of lithium dendrites through the alloying reactions. Furthermore, the volume expansion during the alloying reactions may create pressure steric hindrance, further suppressing the growth of lithium dendrites. As a result, the growth of lithium dendrites can be effectively suppressed through alloying reactions. Accordingly, the design and construction of polymer electrolyte-Si@SiO_x is an effective approach for obtaining dendrite-free lithium metal batteries.

The surface of Si nanoparticles was modified by a layer of PVP to prevent the reaction between the Si nanoparticles and the lithium metal (Figure S1, Supporting Information). Additionally, with the coating of PVP, Si nanoparticles can

https://doi.org/10.1021/acsaem.3c01498
ACS Appl. Energy Mater. 2023, 6, 9523−9531

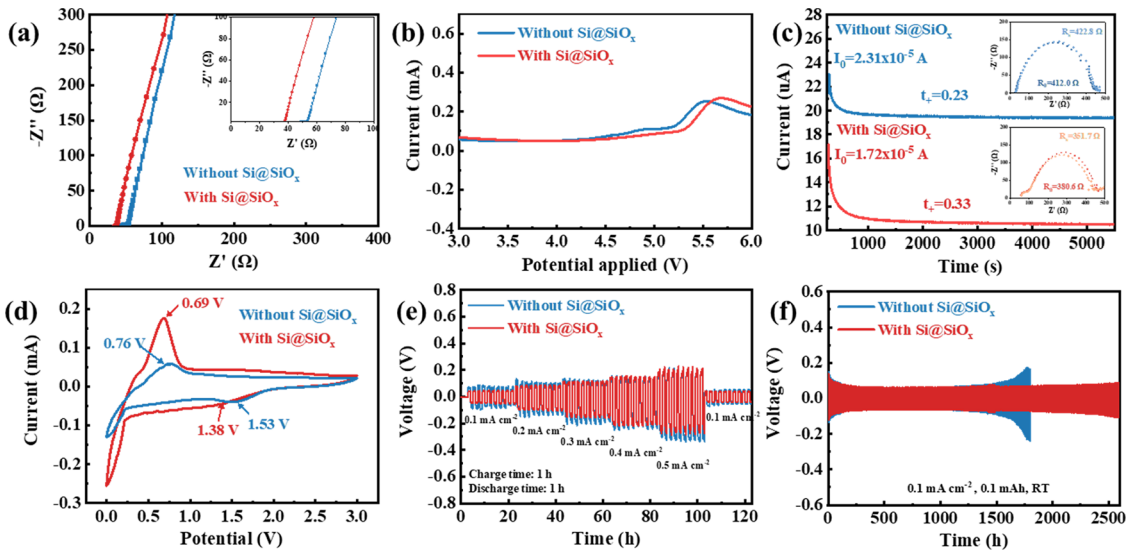

Figure 3. Electrochemical characterization of cells with polymer electrolyte-Si@SiO_x. (a) Electrochemical impedance spectroscopy (EIS) plots of polymer electrolyte-Si@SiO_x. (b) LSV curves of polymer electrolyte-Si@SiO_x. (c) Current−time curves of polymer electrolyte-Si@SiO_x in symmetric Li//Li cells. (d) CV plots of polymer electrolyte-Si@SiO_x at 0.1 mV s^{-1}. (e) Rate performances of polymer electrolyte-Si@SiO_x in symmetric Li//Li cells. (f) Cycling performance of symmetric Li//Li cells of polymer electrolyte-Si@SiO_x at a current density of 0.1 mA cm^{-2}.

be isolated from the contact with air. Thus, a layer of PVP on the surface of Si nanoparticles can reduce the oxidation degree of Si nanoparticles in the air. To characterize the PVP layer, infrared spectroscopy was conducted, as shown in Figure 2a. Compared to Si nanoparticles, the infrared spectra of Si nanoparticles with PVP show absorption peaks at 1684 cm^{-1} (C═O) as well as 2919 and 2960 cm^{-1} ($-CH_3$), reflecting the presence of PVP coating on the surface of Si nanoparticles.[29,30] Besides, TEM imaging was used to analyze the thickness of the PVP layer, which reveals a thickness of approximately 2 nm on the surface of the Si crystals (Figure 2k). The above results suggest that the Si nanoparticles were successfully coated with PVP.

PVP layer can effectively inhibit the reaction between Si nanoparticles and the lithium metal anode, but PVP after swelling in the liquid electrolyte cannot protect Si nanoparticles from reacting with the liquid electrolyte.[31] The Si nanoparticles react with the liquid electrolyte to form a protective film.[32] The protective film can hinder the transfer of lithium ions, which affects the inhibitory effect on lithium dendrites.[26] The appearance of characteristic peaks of Si at 521 and 950 cm^{-1} in the Raman spectra indicates that Si nanoparticles were not oxidized under the protection of PVP at room temperature (Figure 2b).[24] To prevent the reaction between Si nanoparticles and liquid electrolytes, a layer of SiO_x was built at the interface between Si and PVP by oxidizing Si nanoparticles at high temperatures. XRD (Figure 2c) was used to analyze the composition of samples after high-temperature treatment, revealing the absence of SiO_x characteristic peaks. This could be attributed to the amorphous phase and low concentration of SiO_x in the sample, which make it difficult to be detected by XRD.[33] Hence, XPS analysis was conducted (Figure 2d−f), and SiO_x (≈532.2 eV) is shown in Figure 2e, while Si (≈98.7 eV), SiO_2 (≈103.4 eV), $SiO_{1.24}$ (≈102.2 eV), and SiO_x (≈100.8 eV) are also shown in Figure 2f, indicating that Si was oxidized during the high-temperature process.[4,34] The results show that Si nanoparticles were oxidized to form Si@SiO_x nanoparticles with a core−shell structure. The low reactivity of SiO_x with the liquid electrolyte contributes to the great stability of the Si layer in the liquid electrolyte.[34] Si@SiO_x nanoparticles are inorganic materials that do not conduct electrons,[16,35,36] preventing the reaction between Si@SiO_x nanoparticles and lithium ions (Figure S2, Supporting Information).

Thus, the layer of SiO_x is formed at the interface between Si nanoparticles and PVP as a protective barrier for the Si nanoparticles. The stability of the Si@SiO_x layer is important to ensure the stability of the battery performance at the initial stage. The Si@SiO_x nanoparticles react with lithium ions to form a Li−Si alloy after the generation of lithium dendrites. The lithium ions are consumed in the Li−Si alloy reaction, and most of the lithium ions cannot undergo delithiation. Thus, the Coulomb efficiency of the battery is decreased.

The uniform distribution of Si@SiO_x nanoparticles on the surface of polymer electrolytes determines their effectiveness as dendrite stoppers. Different dispersants were used to disperse Si@SiO_x nanoparticles. Compared with other dispersants, PVP can enable the uniform distribution of Si@SiO_x nanoparticles on the surface of the polymer electrolyte (Figures S3 and S4, Supporting Information). SEM images show the uniform distribution of Si@SiO_x nanoparticles, and the surface of the polymer electrolyte is entirely covered by the Si@SiO_x layer (Figure 2g−i). Furthermore, the EDS mapping also confirms the uniform distribution of Si@SiO_x nanoparticles on the surface of the polymer electrolyte (Figure S5, Supporting Information). The uniform dispersion of Si@SiO_x nanoparticles in PVP is due to the existence of lone-pair electrons in the N and O atoms of PVP, which facilitates the coordination bonds with the Si@SiO_x nanoparticles. Besides, PVP as a binder exhibits remarkable compatibility with polymer electrolytes.[31] Therefore, Si@SiO_x nanoparticles can be firmly coated onto the surface of the polymer electrolyte, forming a uniform and stable Si@SiO_x layer. Furthermore, the thickness of the Si@SiO_x layer also has an important effect on the inhibition of lithium dendrites. An excessively thin Si@SiO_x layer fails to suppress the growth of lithium dendrites, whereas a thick layer hinders the transfer of lithium ions. The cross-sectional SEM image of polymer electrolyte-Si@SiO_x

https://doi.org/10.1021/acsaem.3c01498
ACS Appl. Energy Mater. 2023, 6, 9523−9531

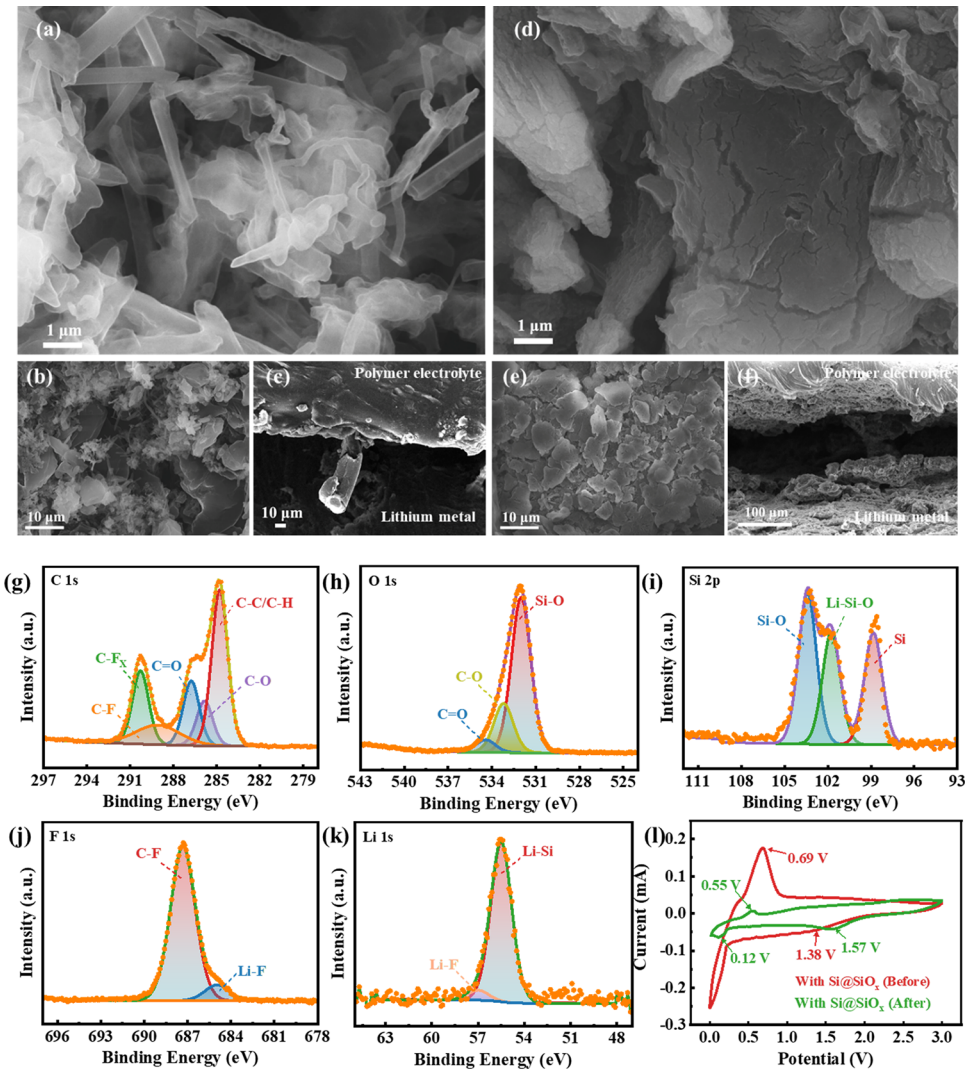

Figure 4. Mechanism analysis of the Si@SiO_x layer acting as a lithium dendrite stopper. (a,b) SEM images of the lithium metal surface of the polymer electrolyte cells. (c) Cross-sectional SEM image of the polymer electrolyte. (d,e) SEM images of the lithium metal surface of the polymer electrolyte-Si@SiO_x cells. (f) Cross-sectional SEM image of polymer electrolyte-Si@SiO_x. (g–k) XPS spectra of the (g) C 1s, (h) O 1s, (i) Si 2p, (j) F 1s, and (k) Li 1s core regions of polymer electrolyte-Si@SiO_x after the cycle. (l) CV plots of polymer electrolyte-Si@SiO_x before and after the cycle at 0.1 mV s^{-1}.

(Figures 2j and S6, Supporting Information) reveals that the thickness of the Si@SiO_x layer is approximately 2 μm. No lithium dendrites are observed on the surface of the lithium metal in cells containing polymer electrolyte-Si@SiO_x after cycling. The symmetric Li//Li cell with the polymer electrolyte-2 μm Si@SiO_x exhibits cycling stability for 2600 h with a polarization voltage of 100 mV, whereas the polymer electrolyte-1 μm Si@SiO_x results in a short circuit at 2560 h, and the polymer electrolyte-4 μm Si@SiO_x shows cycling stability for 1600 h with a polarization voltage of 130 mV (Figure S7, Supporting Information). The results suggest that the polymer electrolyte with a 2 μm Si@SiO_x layer can effectively prevent lithium dendrites and exhibits excellent battery stability. In addition, the Si@SiO_x layer on the surface of the polymer electrolyte can withstand bending up to 180 degrees without being damaged or falling off (Figure 2l), which indicates the excellent flexibility of the Si@SiO_x layer and the firm immobilization of the Si@SiO_x layer on the polymer electrolyte. In conclusion, the Si@SiO_x nanoparticles are uniformly distributed on the surface of the polymer electrolyte by PVP, with a thickness of approximately 2 μm.

The uniform distribution of Si@SiO_x nanoparticles on the surface of polymer electrolytes promotes the homogeneous deposition of lithium ions on the surface of the lithium metal anode. To investigate the electrochemical performance of polymer electrolyte-Si@SiO_x, the ionic conductivity was tested by electrochemical impedance spectroscopy (EIS). The ionic conductivity of polymer electrolyte-Si@SiO_x, which contains 30 μL of liquid electrolyte (5.5×10^{-5} S cm^{-1}) at room temperature, is comparable to that of the polymer electrolyte containing 30 μL of liquid electrolyte (4.9×10^{-5} S cm^{-1}) (Figure 3a). The calculation method of ionic conductivity is presented in Table S1 (Supporting Information).[37−39] Moreover, the electrochemical windows of polymer electrolyte-Si@SiO_x and the polymer electrolyte are similar (above 5.1 V), as observed by using linear sweep voltammetry (LSV). This suggests that the Si@SiO_x layer does not affect the electrochemical window (Figure 3b), which could be ascribed to its nonreactivity with the polymer electrolyte and no impact on

https://doi.org/10.1021/acsaem.3c01498
ACS Appl. Energy Mater. 2023, 6, 9523−9531

the structure of the polymer electrolyte. Additionally, the Li^+ transference number (t_{Li+}) of polymer electrolyte-Si@SiO_x is 0.33, while t_{Li+} of the polymer electrolyte is 0.23 (Figure 3c and Table S2, Supporting Information). The high t_{Li+} of polymer electrolyte-Si@SiO_x is due to the presence of N and O in PVP, which have long electron pairs that attract the lithium ions of $LiPF_6$ to form coordination bonds. Therefore, lithium ions with a smaller volume can migrate quickly in the layer of Si@SiO_x. However, PF_6^- with a larger volume is hindered by the polymer chain segments of PVP. Therefore, the quantity of lithium-ion migration in the Si@SiO_x layer is greater than that of PF_6^-, which further widens the gap between cation and anion migration in polymer electrolyte-Si@SiO_x. Thus, PVP can improve the transference number of lithium ions to a certain extent (Figure S8, Supporting Information).

Si@SiO_x remains stable on the surface of the lithium metal due to the PVP coating. This prevents the Si@SiO_x nanoparticles from reacting with lithium ions during the charge/discharge process, thereby maintaining the Coulombic efficiency of the battery. To analyze the stability of the Si@SiO_x layer in the battery, cyclic voltammetry (CV) was performed using $LiFePO_4$ as the cathode and lithium metal as the anode (Figure 3d). The CV curve of polymer electrolyte-Si@SiO_x shows lithiation and delithiation peaks at 1.38 and 0.69 V, respectively. These peaks are consistent with the CV curve of the polymer electrolyte, where the peaks occur at 1.53 and 0.76 V, respectively. Furthermore, the CV curve of polymer electrolyte-Si@SiO_x does not exhibit the characteristic peaks of SiO_2 during lithiation and delithiation, which occur at 0.28 and 1.2 V, respectively.[40−42] Similarly, the absence of lithiation and delithiation peaks of Si at 0.12, 0.36, and 0.52 V[43−45] indicates the initial stability of the Si@SiO_x layer. The redox peak shift is attributed to the Si@SiO_x layer, which affects the interface reaction between the polymer electrolyte and lithium metal, resulting in the formation of a solid−electrolyte interface.[32,46]

The Si@SiO_x layer enhances the stability of the interface between the polymer electrolyte and lithium metal anode by reacting with lithium ions to form Li_ySi to prevent dendrite growth. This reaction reduces the concentration of lithium ions at the sharp ends of lithium dendrites, thereby improving the performance of a battery with a Si@SiO_x layer. The performance of the rate and cycle is tested using symmetric Li//Li cells. The cell with a Si@SiO_x layer in the polymer electrolyte exhibits an improved rate performance from 0.1 to 0.5 mA cm^{-2} (Figure 3e). Symmetric Li//Li cells exhibit instability during cycling when the current is above 0.5 mA cm^{-2}. Moreover, it has been observed that symmetric Li//Li cells containing polymer electrolyte-Si@SiO_x are comparatively more stable than those containing only the polymer electrolyte (Figure S9, Supporting Information). Additionally, cells with polymer electrolyte-Si@SiO_x can cycle stably for 2600 h at 0.1 mA cm^{-2}, whereas cells with the polymer electrolyte only work for 1500 h (Figure 3f). This demonstrates that the Si@SiO_x layer enhances the stability of the interface between the polymer electrolyte and lithium metal anode.

To analyze the mechanism of the Si@SiO_x layer in inhibiting the growth of lithium dendrites, the surfaces of the lithium metal and polymer electrolyte were characterized by SEM, following cell cycling. Lithium dendrites are observed on the surface of the lithium metal when using a polymer electrolyte in the cells (Figure 4a,b). The cross-sectional SEM image shows that lithium dendrites penetrate polymer electrolytes (Figure 4c). The uneven growth of lithium dendrites in both horizontal and vertical directions on the surface of the lithium metal affects the performance of the cells. The formation of lithium dendrites not only consumes many lithium ions but also creates numerous nonactive sites on the surface of the lithium metal, which leads to the nonuniform deposition of lithium ions and compromises battery safety. In contrast, using polymer electrolyte-Si@SiO_x prevents the formation of lithium dendrites on the surface of the lithium metal in the cells (Figure 4d,e). The absence of lithium dendrites is confirmed by the cross-sectional SEM image (Figure 4f). Furthermore, when the current density of symmetric Li//Li cell is doubled, the Si@SiO_x layer can still inhibit the growth of lithium dendrites (Figure S10, Supporting Information). Further, the lithium dendrites were not present on the surface of Cu in Li/Cu cells with polymer electrolyte-Si@SiO_x, while they existed on the surface of Cu in Li/Cu cells with the polymer electrolyte. The results are consistent with the symmetric Li//Li cell test results, indicating that Si@SiO_x has a good inhibitory effect on lithium dendrites (Figure S11, Supporting Information). In addition, the Si element is uniformly dispersed on the surface of the lithium metal, suggesting that the deposition of lithium ions is induced by the Li−Si alloy reaction to grow in the *xy*-direction (2D growth). Therefore, the coating of the Si@SiO_x layer on the surface of the polymer electrolyte can hinder the growth of lithium ions in the *z*-direction. More importantly, the volume expansion of the Si@SiO_x nanoparticles exerts pressure during the Li−Si alloying reaction to further inhibit the growth of lithium ions in the *z*-direction. Thus, the deposits of lithium ions only show 2D growth to form a pancake-like surface of the lithium metal (Figure S12, Supporting Information). Besides, Si@SiO_x spherical nanoparticles are present in polymer electrolyte-Si@SiO_x before cell cycles, but they are absent after cell cycles (Figure S13, Supporting Information). This suggests that the volume expansion of Si@SiO_x is caused by the Li−Si alloying reaction. These results demonstrate that the alloying reaction can inhibit the growth of lithium dendrites. Further, the volume expansion of Si@SiO_x may have a certain synergistic effect in inhibiting the formation of lithium dendrites.

To further investigate the process of Si@SiO_x nanoparticles inhibiting the growth of lithium dendrites, XPS analysis was conducted to confirm the alloying reaction process. The Si@SiO_x nanoparticles undergo a reaction with the deposited lithium ions and electrons, resulting in the formation of Li_ySi (Figure 4g−k). SiO_x (≈532.10 eV) is observed (Figure 4h) in polymer electrolyte-Si@SiO_x in the cell after cycling, while Figure 4i shows Si (≈98.90 eV), SiO_x (≈103.30 eV), and Li_ySiO_x (≈101.90 eV). Additionally, Li_ySi (≈55.50 eV) is detected in Figure 4k.[4] The presence of Li_ySi and Li_ySiO_x on the surface of polymer electrolyte-Si@SiO_x indicates the occurrence of an alloying reaction between lithium ions and Si@SiO_x. The electrons participating in the reaction are transferred through lithium dendrites. Hence, the layer of Si@SiO_x acts as a stopper for lithium dendrites. Besides, the continued existence of Si@SiO_x at the interface demonstrates its strong alloying capability in effectively suppressing the lithium dendrite growth.

To characterize the layer of Si@SiO_x as a barrier to prevent the formation of lithium dendrites, CV was conducted to analyze this process. Compared with the CV curve of polymer electrolyte-Si@SiO_x before cycling, the CV curve of polymer electrolyte-Si@SiO_x after cycling shows a peak at 0.12 V

https://doi.org/10.1021/acsaem.3c01498
ACS Appl. Energy Mater. 2023, 6, 9523−9531

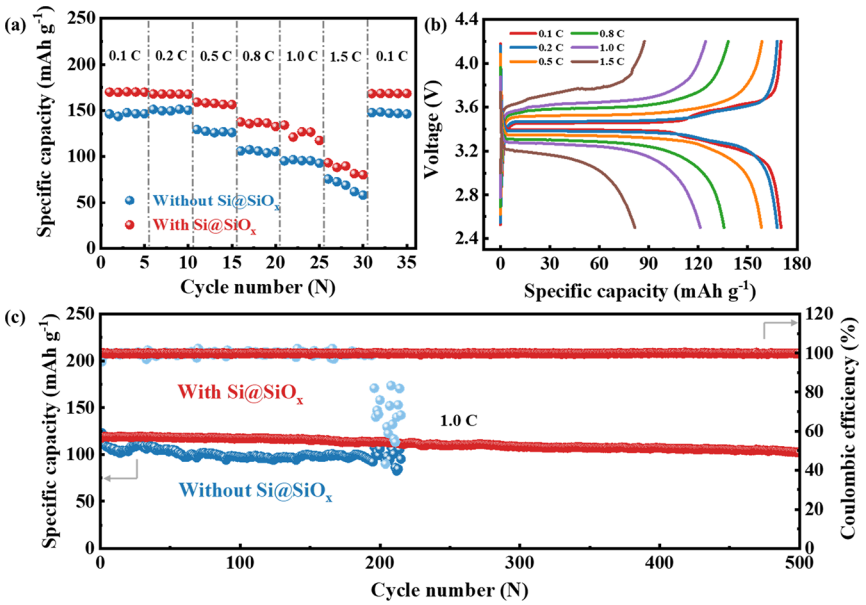

Figure 5. Electrochemical performance of the batteries based on polymer electrolyte-Si@SiO_x. (a) Rate performance of the battery based on polymer electrolyte-Si@SiO_x. (b) Charge−discharge curve of the battery based on polymer electrolyte-Si@SiO_x. (c) Cycling performance of the battery based on polymer electrolyte-Si@SiO_x.

(Figure 4l). The peak at 0.12 V is close to the characteristic intercalation lithium peak (≈0.12 V) of the Si anode.[43] Thus, the CV results suggest that the Li−Si alloying reaction has occurred. The alloying reaction of the Si@SiO_x nanoparticles reduces the concentration of lithium ions, effectively inhibiting the growth of lithium dendrites. Therefore, the Si@SiO_x layer has been demonstrated as an effective dendrite stopper.

The above results have indicated that polymer electrolyte-Si@SiO_x can effectively promote the uniform deposition of lithium ions and form a stable interface. To verify the effect of polymer electrolyte-Si@SiO_x in the full batteries, $LiFePO_4$|| polymer electrolyte-Si@SiO_x||Li battery is carried out in this study, with a range of rates from 0.1 to 1.5 C (Figure 5a,b). The rate performance of the polymer electrolyte-Si@SiO_x-based battery is more stable than that of the polymer electrolyte-based battery. $LiFePO_4$||polymer electrolyte-Si@SiO_x||Li battery maintains a remarkable capacity retention of 86.8% after 500 cycles at 1.0 C, with an average Coulombic efficiency of 99.8% (Figure 5c), while the $LiFePO_4$||polymer electrolyte||Li battery only achieves up to 200 cycles and shows unstable Coulombic efficiency. Thus, the utilization of polymer electrolyte-Si@SiO_x can improve the performance of the full battery. It can be concluded that the polymer electrolyte-Si@SiO_x layer inhibits the growth of lithium dendrites and enhances the stability of the interface between the polymer electrolyte and the lithium metal anode.

4. CONCLUSIONS

In this study, we have demonstrated that the Si@SiO_x nanoparticles on the polymer electrolytes can react with lithium ions deposited at the contact interface to form Li_ySi as a lithium dendrite stopper. The formation of Li_ySi on active sites reduces the concentration of lithium ions, leading to a more uniform lithium-ion concentration between the polymer electrolyte and the lithium metal anode. Hence, a stable interface is formed by the uniform deposition of lithium ions, which inhibits the growth of lithium dendrites. As a result, symmetric Li//Li cells maintain stability without lithium dendrites for more than 2600 h at 0.1 mA cm^{-2}. The $LiFePO_4$|| polymer electrolyte-Si@SiO_x||Li battery maintains a remarkable capacity retention of 86.8% after 500 cycles at 1.0 C, with an average Coulombic efficiency of 99.8%. This study converts the limitations of Si@SiO_x into advantages, significantly expanding its potential applications. Consequently, the Si@SiO_x layer offers a novel alternative solution for addressing the issue of lithium dendrites.

■ ASSOCIATED CONTENT

Supporting Information

The Supporting Information is available free of charge at https://pubs.acs.org/doi/10.1021/acsaem.3c01498.

Additional materials' information, material characterization, and electrochemical data (PDF)

■ AUTHOR INFORMATION

Corresponding Author

Lin Xu − *State Key Laboratory of Advanced Technology for Materials Synthesis and Processing, School of Materials Science and Engineering, Wuhan University of Technology, Wuhan 430070, China; Hubei Longzhong Laboratory, Wuhan University of Technology (Xiangyang Demonstration Zone), Xiangyang 441000 Hubei, China; Hainan Institute, Wuhan University of Technology, Sanya 572000, China;* orcid.org/0000-0003-2347-288X; Email: linxu@whut.edu.cn

Authors

Li Zhao − *State Key Laboratory of Advanced Technology for Materials Synthesis and Processing, School of Materials Science and Engineering, Wuhan University of Technology, Wuhan 430070, China*

Lulu Du − *State Key Laboratory of Advanced Technology for Materials Synthesis and Processing, School of Materials Science and Engineering, Wuhan University of Technology, Wuhan 430070, China*

Hantao Xu − *State Key Laboratory of Advanced Technology for Materials Synthesis and Processing, School of Materials Science and Engineering, Wuhan University of Technology, Wuhan 430070, China*

Jiahui Deng − *State Key Laboratory of Advanced Technology for Materials Synthesis and Processing, School of Materials Science and Engineering, Wuhan University of Technology, Wuhan 430070, China*

Complete contact information is available at: https://pubs.acs.org/10.1021/acsaem.3c01498

Author Contributions

L.Z. and L.D. contributed equally to this work. All authors have given approval to the final version of the manuscript.

Notes

The authors declare no competing financial interest.

■ ACKNOWLEDGMENTS

This work was supported by the National Natural Science Foundation of China (52272234), the National Key Research and Development Program of China (2020YFA0715000), the Key Research and Development Program of Hubei Province (2021BAA070), independent Innovation Projects of the Hubei Longzhong Laboratory (2022ZZ-20), and the Sanya Science and Education Innovation Park of Wuhan University of Technology (2021KF0011).

■ REFERENCES

(1) Zhou, Q.; Yang, X.; Xiong, X.; Zhang, Q.; Peng, B.; Chen, Y.; Wang, Z.; Fu, L.; Wu, Y. A Solid Electrolyte Based on Electrochemical Active $Li_4Ti_5O_{12}$ with PVDF for Solid State Lithium Metal Battery. *Adv. Energy Mater.* **2022**, *12*, 2201991−2202001.

(2) Zheng, Y.; Yang, N.; Gao, R.; Li, Z. Q.; Dou, H. Z.; Li, G. R.; Qian, L. T.; Deng, Y. P.; Liang, J. Q.; Yang, L. X.; Liu, Y. Z.; Ma, Q. Y.; Luo, D.; Zhu, N.; Li, K. C.; Wang, X.; Chen, Z. W. "Tree-Trunk" Design for Flexible Quasi-Solid-State Electrolytes with Hierarchical Ion-Channels Enabling Ultralong-Life Lithium-Metal Batteries. *Adv. Mater.* **2022**, *34*, No. 2203417.

(3) Li, Z.; Wu, G.; Yang, Y.; Wan, Z.; Zeng, X.; Yan, L.; Wu, S.; Ling, M.; Liang, C.; Hui, K. N.; Lin, Z. An Ion-Conductive Grafted Polymeric Binder with Practical Loading for Silicon Anode with High Interfacial Stability in Lithium-Ion Batteries. *Adv. Energy Mater.* **2022**, *12*, No. 2201197.

(4) Liang, H. P.; Zarrabeitia, M.; Chen, Z.; Jovanovic, S.; Merz, S.; Granwehr, J.; Passerini, S.; Bresser, D. Polysiloxane-Based Single-Ion Conducting Polymer Blend Electrolyte Comprising Small-Molecule Organic Carbonates for High-Energy and High-Power Lithium-Metal Batteries. *Adv. Energy Mater.* **2022**, *12*, No. 2200013.

(5) Lee, B. S.; Oh, S.-H.; Choi, Y. J.; Yi, M.-J.; Kim, S. H.; Kim, S.-Y.; Sung, Y.-E.; Shin, S. Y.; Lee, Y.; Yu, S.-H. SiO-induced thermal instability and interplay between graphite and SiO in graphite/SiO composite anode. *Nat. Commun.* **2023**, *14*, 150.

(6) Shen, X.; Zhang, X.-Q.; Ding, F.; Huang, J.-Q.; Xu, R.; Chen, X.; Yan, C.; Su, F.-Y.; Chen, C.-M.; Liu, X.; Zhang, Q. *Energy Mater. Adv.* **2021**, *2021*, No. 1205324.

(7) Meng, X.; Lau, K. C.; Zhou, H.; Ghosh, S. K.; Benamara, M.; Zou, M. Molecular Layer Deposition of Crosslinked Polymeric Lithicone for Superior Lithium Metal Anodes. *Energy Mater. Adv.* **2021**, *2021*, No. 9786201.

(8) Chang, Z.; Yang, H.; Zhu, X.; He, P.; Zhou, H. A stable quasi-solid electrolyte improves the safe operation of highly efficient lithium-metal pouch cells in harsh environments. *Nat. Commun.* **2022**, *13*, 1510−1522.

(9) Chai, S.; Zhang, Y.; Wang, Y.; He, Q.; Zhou, S.; Pan, A. Biodegradable composite polymer as advanced gel electrolyte for quasi-solid-state lithium-metal battery. *eScience* **2022**, *2*, 494−508.

(10) Dong, R.; Wu, F.; Bai, Y.; Li, Q.; Yu, X.; Li, Y.; Ni, Q.; Wu, C. Tailoring Defects in Hard Carbon Anode towards Enhanced Na Storage Performance. *Energy Mater. Adv.* **2022**, *2022*, No. 9896218.

(11) Jung, A.; Lee, M. J.; Lee, S. W.; Cho, J.; Son, J. G.; Yeom, B. Phase Separation-Controlled Assembly of Hierarchically Porous Aramid Nanofiber Films for High-speed Lithium-Metal Batteries. *Small* **2022**, *18*, No. e2205355.

(12) Liu, H.-J.; Qu, J.; Chang, Y.; Yang, C.-Y.; Zhai, X.-Z.; Yu, Z.-Z.; Li, X. Engineering Lithiophilic Silver Sponge Integrated with Ion-Conductive PVDF/LiF Protective Layer for Dendrite-Free and High-Performance Lithium Metal Batteries. *ACS Appl. Energy Mater.* **2023**, *6*, 519−529.

(13) He, Y.; Zhang, M.; Wang, A.; Zhang, B.; Pham, H.; Hu, Q.; Sheng, L.; Xu, H.; Wang, L.; Park, J.; He, X. Regulation of Dendrite-Free Li Plating via Lithiophilic Sites on Lithium-Alloy Surface. *ACS Appl. Mater. Interfaces* **2022**, *14*, 33952−33959.

(14) You, Y.; Zheng, F.; Zhang, D.; Zhao, C.; Hu, C.; Cao, X.; Zhu, Z.-z.; Wu, S. Effect of Charge Non-Uniformity on the Lithium Dendrites and Improvement by the LiF Interfacial Layer. *ACS Appl. Energy Mater.* **2022**, *5*, 15078−15085.

(15) Pathak, R.; Chen, K.; Gurung, A.; Reza, K. M.; Bahrami, B.; Pokharel, J.; Baniya, A.; He, W.; Wu, F.; Zhou, Y.; Xu, K.; Qiao, Q. Fluorinated hybrid solid-electrolyte-interphase for dendrite-free lithium deposition. *Nat. Commun.* **2020**, *11*, 93−104.

(16) Duan, C.; Cheng, Z.; Li, W.; Li, F.; Liu, H.; Yang, J.; Hou, G.; He, P.; Zhou, H. Realizing the compatibility of a Li metal anode in an all-solid-state Li−S battery by chemical iodine−vapor deposition. *Energy Environ. Sci.* **2022**, *15*, 3236−3245.

(17) Cao, W.; Li, Q.; Yu, X.; Li, H. Controlling Li deposition below the interface. *eScience* **2022**, *2*, 47−78.

(18) Li, Y.; Hu, A.; Gan, X.; He, M.; Zhu, J.; Chen, W.; Hu, Y.; Lei, T.; Li, F.; Li, Y.; Fan, Y.; Wang, F.; Zhou, M.; Wen, A.; Li, B. Synergy of in-situ heterogeneous interphases tailored lithium deposition. *Nano Res.* **2023**, *16*, 8304.

(19) Zhao, Q.; Zhou, R.; Wang, C.; Kang, J.; Zhang, Q.; Liu, J.; Jin, Y.; Wang, H.; Zheng, Z.; Guo, L. Anion Immobilization Enabled by Cation-Selective Separators for Dendrite-Free Lithium Metal Batteries. *Adv. Funct. Mater.* **2022**, *32*, 2112711−2112721.

(20) Mouraliraman, D.; Shaji, N.; Praveen, S.; Nanthagopal, M.; Ho, C. W.; Karthik, M. V.; Kim, T.; Lee, C. W. Thermally Stable PVDF-HFP-Based Gel Polymer Electrolytes for High-Performance Lithium-Ion Batteries. *Nanomaterials* **2022**, *12*, 1056.

(21) Shi, Y.; Wan, J.; Liu, G. X.; Zuo, T. T.; Song, Y. X.; Liu, B.; Guo, Y. G.; Wen, R.; Wan, L. J. Interfacial Evolution of Lithium Dendrites and Their Solid Electrolyte Interphase Shells of Quasi-Solid-State Lithium-Metal Batteries. *Angew. Chem., Int. Ed.* **2020**, *59*, 18120−18125.

(22) He, R.; Wang, Y.; Zhang, C.; Liu, Z.; He, P.; Hong, X.; Yu, R.; Zhao, Y.; Wu, J.; Zhou, L.; Mai, L. Sequential and Dendrite-Free Li Plating on Cu Foil Enabled by an Ultrathin Yolk−Shell SiO_x/C@C Layer. *Adv. Energy Mater.* **2023**, *13*, No. 2204075.

(23) Entwistle, J. E.; Booth, S. G.; Keeble, D. S.; Ayub, F.; Yan, M.; Corr, S. A.; Cumming, D. J.; Patwardhan, S. V. Insights into the Electrochemical Reduction Products and Processes in Silica Anodes for Next-Generation Lithium-Ion Batteries. *Adv. Energy Mater.* **2020**, *10*, No. 2001826.

(24) Park, J. B.; Choi, C.; Yu, S.; Chung, K. Y.; Kim, D. W. Porous Lithiophilic Li−Si Alloy-Type Interfacial Framework via Self-Discharge Mechanism for Stable Lithium Metal Anode with Superior Rate. *Adv. Energy Mater.* **2021**, *11*, 2101544−2101558.

(25) Zhao, P.; Kuang, G.; Qiao, R.; Liu, K.; Boorboor Ajdari, F.; Sun, K.; Bao, C.; Salavati-Niasari, M.; Song, J. Regulating Lithium Ion Transport by a Highly Stretchable Interface for Dendrite-Free Lithium Metal Batteries. *ACS Appl. Energy Mater.* **2022**, *5*, 10141−10148.

(26) Sung, J.; Kim, N.; Ma, J.; Lee, J. H.; Joo, S. H.; Lee, T.; Chae, S.; Yoon, M.; Lee, Y.; Hwang, J.; Kwak, S. K.; Cho, J. Subnano-sized silicon anode via crystal growth inhibition mechanism and its application in a prototype battery pack. *Nat. Energy* **2021**, *6*, 1164−1175.
(27) Zhang, X.; Cui, Z.; Manthiram, A. Insights into the Crossover Effects in Cells with High-Nickel Layered Oxide Cathodes and Silicon/Graphite Composite Anodes. *Adv. Energy Mater.* **2022**, *12*, No. 2103611.
(28) Huang, A.; Ma, Y.; Peng, J.; Li, L.; Chou, S.-l.; Ramakrishna, S.; Peng, S. Tailoring the structure of silicon-based materials for lithium-ion batteries via electrospinning technology. *eScience* **2021**, *1*, 141−162.
(29) Tan, D. H. S.; Banerjee, A.; Chen, Z.; Meng, Y. S. From nanoscale interface characterization to sustainable energy storage using all-solid-state batteries. *Nat. Nanotechnol.* **2020**, *15*, 170−180.
(30) Hwang, J.; Matsumoto, K.; Chen, C.-Y.; Hagiwara, R. Pseudo-solid-state electrolytes utilizing the ionic liquid family for rechargeable batteries. *Energy Environ. Sci.* **2021**, *14*, 5834−5863.
(31) Gonzalez, G.; Hasan, M. T.; Ramirez, D.; Parsons, J.; Alcoutlabi, M. Synthesis of SnO_2/TiO_2 micro belt fibers from polymer composite precursors and their applications in Li-ion batteries*. *Polym. Eng. Sci.* **2022**, *62*, 360−372.
(32) Peled, E.; Schneier, D.; Shaham, Y.; Ardel, G.; Burstein, L.; Kamir, Y. Understanding the Spontaneous Reactions between Oxide-Free Silicon and Lithium-Battery Electrolytes. *J. Electrochem. Soc.* **2019**, *166*, A2091−A2095.
(33) Hu, G.; Zhong, K.; Yu, R.; Liu, Z.; Zhang, Y.; Wu, J.; Zhou, L.; Mai, L. Enveloping SiO_x in N-doped carbon for durable lithium storage via an eco-friendly solvent-free approach. *J. Mater. Chem. A* **2020**, *8*, 13285−13291.
(34) Chen, W.; Salvatierra, R. V.; Ren, M.; Chen, J.; Stanford, M. G.; Tour, J. M. Laser-Induced Silicon Oxide for Anode-Free Lithium Metal Batteries. *Adv. Mater.* **2020**, *32*, No. e2002850.
(35) Huo, H.; Janek, J. Silicon as Emerging Anode in Solid-State Batteries. *ACS Energy Lett.* **2022**, *7*, 4005−4016.
(36) He, X. Z.; Ji, X.; Zhang, B.; Rodrigo, N. D.; Hou, S.; Gaskell, K.; Deng, T.; Wan, H. L.; Liu, S. F.; Xu, J. J.; Nan, B.; Lucht, B. L.; Wang, C. S. Tuning Interface Lithiophobicity for Lithium Metal Solid-State Batteries. *ACS Energy Lett.* **2022**, *7*, 131−139.
(37) Raj, V.; Venturi, V.; Kankanallu, V. R.; Kuiri, B.; Viswanathan, V.; Aetukuri, N. P. B. Direct correlation between void formation and lithium dendrite growth in solid-state electrolytes with interlayers. *Nat. Mater.* **2022**, *21*, 1050−1056.
(38) Sun, J.; Peng, J.; Ring, T.; Whittaker-Brooks, L.; Zhu, J.; Fraggedakis, D.; Niu, J.; Gao, T.; Wang, F. Lithium deposition mechanism on Si and Cu substrates in the carbonate electrolyte. *Energy Environ. Sci.* **2022**, *15*, 5284−5299.
(39) Chen, B.; Chen, L.; Zu, L.; Feng, Y.; Su, Q.; Zhang, C.; Yang, J. Zero-Strain High-Capacity Silicon/Carbon Anode Enabled by a MOF-Derived Space-Confined Single-Atom Catalytic Strategy for Lithium-Ion Batteries. *Adv. Mater.* **2022**, *34*, No. e2200894.
(40) Shatalova, E. I.; Grizanova, E. V.; Dubovskiy, I. M. The Effect of Silicon Dioxide Nanoparticles Combined with Entomopathogenic Bacteria or Fungus on the Survival of Colorado Potato Beetle and Cabbage Beetles. *Nanomaterials* **2022**, *12*, 1558.
(41) Liu, X.; Zhang, T.; Shi, X.; Ma, Y.; Song, D.; Zhang, H.; Liu, X.; Wang, Y.; Zhang, L. Hierarchical Sulfide-Rich Modification Layer on SiO/C Anode for Low-Temperature Li-Ion Batteries. *Adv. Sci.* **2022**, *9*, No. e2104531.
(42) Li, C.-L.; Huang, G.; Yu, Y.; Xiong, Q.; Yan, J.-M.; Zhang, X.-B. Three Birds with One Stone: An Integrated Cathode-Electrolyte Structure for High-Performance Solid-State Lithium-Oxygen Batteries. *Small* **2022**, *18*, No. e2107833.
(43) Xiong, J.; Dupré, N.; Moreau, P.; Lestriez, B. From the Direct Observation of a PAA-Based Binder Using STEM-VEELS to the Ageing Mechanism of Silicon/Graphite Anode with High Areal Capacity Cycled in an FEC-Rich and EC-Free Electrolyte. *Adv. Energy Mater.* **2022**, *12*, No. 2103348.
(44) Adhitama, E.; van Wickeren, S.; Neuhaus, K.; Frankenstein, L.; Demelash, F.; Javed, A.; Haneke, L.; Nowak, S.; Winter, M.; Gomez-Martin, A.; Placke, T. Revealing the Role, Mechanism, and Impact of AlF_3 Coatings on the Interphase of Silicon Thin Film Anodes. *Adv. Energy Mater.* **2022**, *12*, No. 2201859.
(45) Adhitama, E.; Dias Brandao, F.; Dienwiebel, I.; Bela, M. M.; Javed, A.; Haneke, L.; Stan, M. C.; Winter, M.; Gomez-Martin, A.; Placke, T. Pre-Lithiation of Silicon Anodes by Thermal Evaporation of Lithium for Boosting the Energy Density of Lithium Ion Cells. *Adv. Funct. Mater.* **2022**, *32*, 2201455−2201469.
(46) Liu, Y.; Tao, X.; Wang, Y.; Jiang, C.; Ma, C.; Sheng, O.; Lu, G.; Lou, X. W. D. Self-assembled monolayers direct a LiF-rich interphase toward long-life lithium metal batteries. *Science* **2022**, *375*, 739−745.

https://doi.org/10.1021/acsaem.3c01498
ACS Appl. Energy Mater. 2023, 6, 9523−9531